Electromagnetic Properties of Nuclei Calculated from Projected Hartree-Fock Wave Functions

M. R. GUNYE*
Bhabha Atomic Research Centre, Trombay, Bombay, India

AND

CHINDHU S. WARKE
Tata Institute of Fundamental Research, Colaba, Bombay, India

(Received 20 March 1967)

Using the projected Hartree-Fock (HF) wave functions, a theoretical formulation is given for calculating the electromagnetic properties of nuclei, the nuclear form factors in electron scattering, ft values in β decay, and the reduced widths of nuclear levels in direct reactions. The formulation is applied to calculate the quadrupole and magnetic moments, the electromagnetic transition probabilities, and the lifetimes of nuclear levels of a large number of nuclei ranging from ^{19}F to ^{37}Cl in the $2s$-$1d$ shell. The good agreement between the calculated and the experimental values indicates a remarkable success of the projected HF wave functions in predicting the electromagnetic properties of nuclei.

I. INTRODUCTION

THERE are two main difficulties that arise in the development of the theory of finite nuclei. The first concerns the strong short-range nature of nuclear forces, and the other the finite size of nuclei. Some attempts have been made to overcome these difficulties.[1] However, these methods could not be used for all the nuclei because of their intrinsic difficulties. The first difficulty is in obtaining an effective interaction in shell-model calculations for nucleons outside the core.[2] The second difficulty is in constructing antisymmetric states of good angular momentum for many-nucleon systems. We know that the shell model works very well, and hence any basic theory should finally lead to it.

We avoid the first difficulty by assuming a phenomenological internucleon interaction in the Hartree-Fock (HF) calculations for nucleons outside the core. Our essential aim is to find an approximation which can overcome the second difficulty in the exact treatment of the many-body finite system. This is equivalent to finding a workable method which can reproduce reasonable results for a set of nuclei without requiring a simplified model. Of course the shell-model configuration-mixing calculation is an alternative approach,[3] but this method is rather difficult to handle in the case of many-nucleon systems. The projection technique[4] (an approximation to the configuration-mixing calculation) is what we will be investigating further. Our earlier studies[5] show that it reproduces the binding energies and the low-lying excited spectra quite well. However, we know that these quantities are rather insensitive to the wave functions.

In this paper, we develop a formalism to test wave functions obtained from the HF state by a projection prescription. If one has to test the wave function, one should choose a probe which has a known interaction with the nucleus. The interaction between the probe and the nucleus under study does not have to be assumed, because this assumption would make it difficult to test the nuclear wave function. Though electromagnetic properties of the nucleus depend on what the nuclear currents and densities (effective changes) are, there are some physical grounds for their proper choice.[6] We can use these properties in testing nuclear wave functions. Besides these, other tests that one could carry out are the nuclear form factors in electron scattering, ft values in β decay, and single-particle reduced widths in direct reactions. We discuss the theoretical formulation of all these tests. As an application of this theory, we have calculated magnetic moments, quadrupole moments, and transition probabilities for the nuclei in the $2s$-$1d$ shell.

II. THEORETICAL FORMULATION

In this paper we will not rewrite the expression derived in Ref. 5 for the evaluation of

$$p_{K'K}{}^{I}(A)=\langle\phi_{K'}|P_{K'K}{}^{I}|\phi_{K}\rangle, \qquad (1)$$

where $P_{K'K}{}^{I}$ is the projection operator defined in Ref. 5; $\phi_{K'}$ and ϕ_{K} $(=|K\rangle)$ are the HF determinantal states

* Correspondence address: Tata Institute of Fundamental Research, Colaba, Bombay 5, India.

[1] K. A. Brueckner, J. L. Gammel, and H. Weitzner, Phys. Rev. **110**, 431 (1958); S. A. Moszkowski and B. L. Scott, Ann. Phys. **11**, 657 (1960); R. K. Bhaduri and E. L. Townsiak, Proc. Phys. Soc. (London) **86**, 451 (1965); C. Shakin and Y. R. Waghmare, Phys. Rev. Letters **16**, 403 (1966).

[2] T. S. Kuo and G. E. Brown, Nucl. Phys. **85**, 40 (1966).

[3] J. P. Elliot and B. M. Flowers, Proc. Roy. Soc. (London) **A229**, 536 (1955).

[4] M. Redlich, Phys. Rev. **110**, 468 (1958); D. Kurath and L. Picman, Nucl. Phys. **10**, 313 (1959); M. K. Banerjee and C. A. Levinson, Phys. Rev. **130**, 1036 (1963); W. H. Bassichis and G. Ripka, Phys. Letters **15**, 320 (1965); W. H. Bassichis, B. Girand, and G. Ripka, Phys. Rev. Letters **13**, 52 (1965); I. Unna, Phys. Rev. **132**, 2225 (1963); I. Kelson, Nucl. Phys. **89**, 387 (1966).

[5] C. S. Warke and M. R. Gunye, Phys. Rev. **155**, 1084 (1967); M. R. Gunye and C. S. Warke, *ibid.* **156**, 1087 (1967).

[6] B. Mottelson, *Cours de l'Ecole d'Ete de Physique Théorique des Houches* (Dunod Cie., Paris, 1959); M. R. Gunye and S. Das Gupta, Nucl. Phys. **89**, 443 (1966).

of given number A of nucleons. We first calculate the matrix element $\langle\Psi_{M'K'}{}^{I'}|T_\mu{}^\lambda|\Psi_{MK}{}^I\rangle$ of a general one-body tensor operator

$$T_\mu{}^\lambda=\sum_{i=1}^{A} T_\mu{}^\lambda(i)$$

between the states $\Psi_{M'K'}{}^{I'}$ and $\Psi_{MK}{}^I$ projected from the HF states $\phi_{K'}$ and ϕ_K respectively. We are employing unnormalized projected states. Using the Wigner-Eckart theorem, we write

$$\langle\Psi_{M'K'}{}^{I'}|T_\mu{}^\lambda|\Psi_{MK}{}^I\rangle=(I\lambda M\mu|I'M')\langle I'K'\|T^\lambda\|IK\rangle, \quad (2)$$

where the first bracket on the right-hand side is the Clebsch-Gordan coefficient for angular momentum coupling, and the second is the many-particle reduced matrix element. Our aim is to evaluate the latter in terms of the single-particle reduced matrix elements and the matrix elements $p_{K'K}{}^I(A-1)$ of $A-1$ particles. It is not difficult to show that

$$\langle\Psi_{M'K'}{}^{I'}|T_\mu{}^\lambda|\Psi_{MK}{}^I\rangle = (I\lambda M\mu|I'M')\sum_{\mu'}(I\lambda K'-\mu'\mu'|I'K') \times\langle K'|T_{\mu'}{}^\lambda P_{K'-\mu',K}{}^I|K\rangle\cdots. \quad (3)$$

From Eqs. (2) and (3) we have

$$\langle I'K'\|T^\lambda\|IK\rangle =\sum_{\mu'}(I\lambda K'-\mu'\mu'|I'K')\langle K'|T_{\mu'}{}^\lambda P_{K'-\mu',K}{}^I|K\rangle. \quad (4)$$

We have explicitly evaluated[5] the expression in Eq. (4); we can, however, simplify it further. Using simple properties of the Clebsch-Gordan coefficients and the projection operator, one can show that

$$\langle I'K'\|T^\lambda\|IK\rangle = (2I+1)^{1/2}\sum_{i,k,J}(-)^{i+k+j_i+I'+J+\lambda}C_{\Omega_i}{}^{j_i}(K)C_{\Omega_k}{}^{j_k}(K') \times(Jj_iK-\Omega_i\Omega_i|IK)(Jj_kK'-\Omega_k\Omega_k|I'K') \times\begin{Bmatrix} I & j_i & J \\ j_k & I' & \lambda \end{Bmatrix}(n_kl_kj_k\|T^\lambda\|n_il_ij_i) \times p_{K'-\Omega_k,K-\Omega_i}{}^J(A-1)\cdots. \quad (5)$$

The summation over i (k) in Eq. (5) indicates a summation both over $n_il_ij_i$ ($n_kl_kj_k$) and over the particles. The reduced matrix element in the right-hand side of Eq. (5) is the single-particle reduced matrix element as defined in Ref. 7, and $C^j(K)$ are the coefficients in the HF solution for the K band. For numerical computation, the expression given in Eq. (5) is the most useful.

As expected, the many-particle reduced matrix element in Eq. (5) has the following property:

$$\frac{\langle I'K'\|T^\lambda\|IK\rangle}{\langle IK\|T^\lambda\|I'K'\rangle}=\left(\frac{2I+1}{2I'+1}\right)^{1/2}\cdots. \quad (6)$$

A. Magnetic Moment, Quadrupole Moment, and Electromagnetic Transition Probability

The operators for the magnetic moment M, the quadrupole moment Q, and the electric and magnetic multipole fields $B_e(\lambda,\mu)$ and $B_m(\lambda,\mu)$ are[7]

$$\mathbf{M}=\tfrac{1}{2}\sum_{i=1}^{A}[(1+\tau_3{}^i)(g_l\mathbf{l}_i+g_s\boldsymbol{\sigma}_i)+(1-\tau_3{}^i)g_s'\boldsymbol{\sigma}_i],$$

$$Q=\tfrac{1}{2}(16\pi/5)^{1/2}\sum_{i=1}^{A}[(1+\tau_3{}^i)e_p +(1-\tau_3{}^i)e_n]r_i{}^2Y_{20}(i),$$

$$B_e(\lambda,\mu)=\tfrac{1}{2}\sum_{i=1}^{A}[(1+\tau_3{}^i)e_p+(1-\tau_3{}^i)e_n]r_i{}^\lambda Y_{\lambda\mu}(i),$$

$$B_m(\lambda,\mu)=\tfrac{1}{2}\sum_{i=1}^{A}\left[(1+\tau_3{}^i)\left(\frac{2}{\lambda+1}g_l\mathbf{l}_i+g_s\boldsymbol{\sigma}_i\right) +(1-\tau_3{}^i)g_s'\boldsymbol{\sigma}_i\right]\cdot\nabla_i[r_i{}^\lambda Y_{\lambda\mu}(i)]\cdots, \quad (7)$$

where e_p and e_n are the effective charges of protons and neutrons; g_l, g_s, and g_s' have the values 1, 2.793, and -1.913, respectively in units of nuclear magnetons. All the operators in Eq. (7) have the form $\sum_i T_\mu{}^\lambda(i)$, and their matrix element with respect to antisymmetric states can be written as

$$\langle\Psi_{M'K'}{}^{I'}|\sum_i T_\mu{}^\lambda(i)|\Psi_{MK}{}^I\rangle = (I\lambda M\mu|I'M')\langle I'K'\|T^\lambda\|IK\rangle.$$

If we know the single-particle reduced matrix elements involved, it is straightforward to calculate, from Eq. (5), the matrix elements of the operators in Eq. (7). We avoid writing the lengthy expressions for each operator; instead we quote[7] the single-particle reduced matrix elements required in the evaluation of the electromagnetic properties of nuclei. Before we give the reduced single-particle matrix elements, we note that our single-particle wave functions ψ_{nljm} are given by

$$\psi_{nljm}=\sum_{m_s}(l\tfrac{1}{2}m-m_sm_s|jm)R_{nl}(r)Y_{l,m-m_s}(\theta,\varphi)\chi_{m_s}\cdots, \quad (8)$$

where $R_{nl}(r)$ is an oscillator radial wave function and χ

[7] A. de-Shalit and I. Talmi, *Nuclear Shell Theory* (Academic Press Inc., New York, 1963).

is the spin function. Then

$$(n'l'j'\|\boldsymbol{\sigma}\|nlj)=\delta_{nn'}\delta_{ll'}(-)^{j'+l-1/2}[6(2j+1)(2j'+1)]^{1/2}\begin{Bmatrix}\frac{1}{2} & \frac{1}{2} & 1\\ j & j' & l\end{Bmatrix},$$

$$(n'l'j'\|\mathbf{l}\|nlj)=\delta_{nn'}\delta_{ll'}(-)^{j+l-1/2}[l(l+1)(2l+1)(2j+1)(2j'+1)]^{1/2}\begin{Bmatrix}l & l & 1\\ j & j' & \frac{1}{2}\end{Bmatrix},$$

$$(n'l'j'\|r^\lambda Y_\lambda\|nlj)=(-)^\lambda[1+(-)^{l+l'+\lambda}][(2\lambda+1)(2j'+1)/16\pi]^{1/2}(j'\lambda\tfrac{1}{2}0|j\tfrac{1}{2})(n'l'\|r^\lambda\|nl), \tag{9}$$

$$(n'l'j'\|\boldsymbol{\sigma}_i\cdot\boldsymbol{\nabla}_i(r_i^\lambda Y_\mu^\lambda(i))\|nlj)=(-)^{l'}(2\lambda+1)[3\lambda(2\lambda-1)(2j+1)(2j'+1)(2l'+1)/2\pi]^{1/2}$$
$$\times(l'\lambda-100|l0)\begin{Bmatrix}l' & \frac{1}{2} & j'\\ l & \frac{1}{2} & j\\ \lambda-1 & 1 & \lambda\end{Bmatrix}(n'l'\|r^{\lambda-1}\|nl),$$

$$(n'l'j'\|\mathbf{j}_i\cdot\boldsymbol{\nabla}_i(r_i^\lambda Y_\mu^\lambda(i))\|nlj)=(-)^{l+j'+1/2}(2\lambda+1)(2j+1)[\lambda(2\lambda-1)j(j+1)(2j'+1)(2l'+1)]^{1/2}$$
$$\times(l'\lambda-100|l0)\begin{Bmatrix}l' & j' & \frac{1}{2}\\ j & l & \lambda-1\end{Bmatrix}\begin{Bmatrix}j' & \lambda & l\\ 1 & j & \lambda-1\end{Bmatrix}(n'l'\|r^{\lambda-1}\|nl).$$

The radial integral in the formulas in Eq. (9) can be readily obtained by using the harmonic-oscillator wave functions[7] and is given by

$$(n'l'\|r^\lambda\|nl)=\left(\frac{\hbar}{M\omega}\right)^{\lambda/2}[(2)^{l+l'-n-n'+2}(2l+2n+1)!!(2l'+2n'+1)!!/(\pi n!n'!)]^{1/2}$$
$$\times\sum_{k=0}^{n}\sum_{k'=0}^{n'}(-2)^{k+k'}\binom{n}{k}\binom{n'}{k'}[(2k+2k'+l+l'+\lambda+1)/2]!/[(2l+2k+1)!!(2l'+2k'+1)!!], \tag{10}$$

where $2n+l=N$, the principal quantum number of the harmonic-oscillator shell, and both n and l take integral values from 0 to the maximum permissible. The notation in Eqs. (9) and (10) is that of Ref. 7.

B. Nuclear Form Factor in Electron Scattering

The inelastic scattering of high-energy electrons provides a useful tool for testing nuclear wave functions. It is known that the effect of the transverse electric interaction can be neglected[8] and that it is enough to consider only the longitudinal Coulomb interaction. Further, since in light nuclei, $e_pZ/137+e_nN/137$ is small (where Z and N are the numbers of protons and neutrons), first Born approximation is enough to calculate the cross sections. It has been pointed out[8] that for excited states characterized by a strong configuration mixing, a Gaussian shape is entirely inadequate for the transition density, which is the overlap between the excited and ground state wave functions. In the relativistic limit, the inelastic differential cross section, with the above approximations, is given by[9]

$$\sigma(\theta)=\sigma_M(\theta)|F(\mathbf{q})|^2, \tag{11}$$

where $\sigma_M(\theta)$, the Mott cross section for the electron of incident energy E_i, is given by

$$\sigma_M(\theta)=e^4\cos^2(\theta/2)/4E_i^2\sin^4(\theta/2),$$

and the form factor $F(\mathbf{q})$ for the momentum transfer $\mathbf{q}$ is given by

$$F(\mathbf{q})=\langle f|\sum_{i=1}^{A}\tfrac{1}{2}[(1+\tau_3{}^i)e_p+(1-\tau_3{}^i)e_n]e^{i\mathbf{q}\cdot\mathbf{r}_i}|i\rangle, \tag{12}$$

where $|i\rangle$ and $|f\rangle$ are the initial- and final-state nuclear wave functions, respectively. Besides the form factor $F(\mathbf{q})$ in Eq. (11), one has to multiply $\sigma_M(\theta)$ by two correction factors: one due to the finite size of the proton and the second due to the center-of-mass correction. By expanding the exponential in Eq. (12) we have

$$F(\mathbf{q})=4\pi\sum_\lambda i^\lambda Y_{\lambda\mu}{}^*(\mathbf{q})F_\mu{}^\lambda(\mathbf{q}),$$

where $F_\mu{}^\lambda(\mathbf{q})$ has a similar structure to that of $B_e(\lambda,\mu)$ except that in this case, the radial integral in Eq. (9) would be $(n_fl_f\|j_\lambda(qr)\|n_il_i)$ instead of $(n_fl_f\|r^\lambda\|n_il_i)$. Using the Hankel transform,[10] it is straightforward to

[8] V. Gillet and M. A. Melkanoff, Phys. Rev. **133**, B1190 (1961).
[9] R. Huby, Rept. Progr. Phys. **21**, 59 (1958).
[10] H. Bateman, *Tables of Integral Transformations* (McGraw-Hill Book Company, Inc., New York, 1954).

carry out the radial integral

$$(n'l'\|j_\lambda(qr)\|nl)=(q/2\sqrt{2}\nu^{1/2})^\lambda\frac{\exp(-q^2/8\nu)}{(\lambda+\frac{1}{2})!}\left[\frac{2^{l+l'-n-n'}(2l+2n+1)!!(2l'+2n'+1)!!}{n!n'!}\right]^{1/2}\sum_{k=0}^{n}\sum_{k'=0}^{n'}(-2)^{k+k'}\binom{n}{k}\binom{n'}{k'}$$
$$\times\left(\frac{2k+2k'+l+l'+1+\lambda}{2}\right)!F\left(\frac{\lambda}{2}-\frac{2k+2k'+l+l'}{2},\lambda+\tfrac{3}{2},q^2/8\nu\right)\Big/(2k+2l+1)!!(2k'+2l'+1)!!, \quad (13)$$

where $F(a,b,z)$ is the hypergeometric function,[10] and the other symbols are the same as in Ref. 7. For the unpolarized target, the cross section in Eq. (11) after summing over final states and averaging over initial states becomes

$$\sigma(\theta)=\sigma_M(\theta)\times 4\pi[(2I'+1)/(2I+1)]\sum_\lambda\langle I'K'\|F^\lambda\|IK\rangle^2. \quad (14)$$

The reduced matrix element in Eq. (14) can be obtained from Eqs. (5) and (9).

C. Single-Particle Reduced Widths in Direct Reactions

It is known[11] that stripping and pickup reactions at low incident deuteron energy also provide a sensitive tool for studying the wave functions of nuclear states through the measurement of their reduced widths. This is firstly because the neutron capture in (d,p) reactions, and the pickup in (d,t) reactions take place at the nuclear surface without the complications of an intermediate compound nucleus, and secondly because they are insensitive to the deuteron-nucleus interaction. Let us define[11] the quantity β_{jl} as follows:

$$\beta_{jl}=\langle\Psi_{M'K'}{}^{I'}(A+1)\,|\sum_m(IjMm\,|\,I'M')\Psi_{MK}{}^I(A)\varphi_m{}^{jl}\rangle, \quad (15)$$

where $\varphi_m{}^{jl}$ is the wave function of the stripped or the captured neutron; $\Psi_{M'K'}{}^{I'}(A+1)$ and $\Psi_{MK}{}^I(A)$ are the wave functions of the nuclei with $A+1$ and A nucleons, respectively. The reduced width is then defined by

$$\theta_{jl}{}^2=(A+1)\beta_{jl}{}^2. \quad (16)$$

We know that the differential cross section depends only on the orbital angular momentum l of the captured or stripped neutron and not on $j=l\pm\frac{1}{2}$. Since the two j values do not interfere, we define S_l, the spectroscopic factor by

$$S_l=\sum_j\theta_{jl}{}^2. \quad (17)$$

In terms of S_l and the intrinsic single-particle cross section $\phi_l(\theta)$, the differential cross section for the stripping or pickup reaction has the form

$$\sigma(\theta)=[(2I'+1)/(2I+1)]\sum_l S_l\phi_l(\theta). \quad (18)$$

In Eq. (18), S_l contains information on the nuclear wave functions. After expanding the determinant of $A+1$ particles into a product of a determinant of A particles and a single-particle orbital, one obtains β_{jl} in Eq. (15):

$$\beta_{jl}=[p_{K'K'}{}^{I'}(A+1)p_{KK}{}^I(A)(A+1)]^{-1/2}\times\sum_{i=1}^{A}(-)^iC_{\Omega_i}{}^{j(l)}(K')(IjK'-\Omega_i\Omega_i\,|\,I'K')\times p_{K'-\Omega_i,K}{}^I(A). \quad (19)$$

A sum rule similar to that in Ref. 11 can easily be derived by using Eq. (19) and noting that $\sum_j(C_{\Omega_i}{}^{j(l)})^2=1$:

$$\sum_{jlI'}p_{K'K}{}^{I'}(A+1)\theta_{jl}{}^2=\sum_i(p_{K'-\Omega_i,K}{}^I(A))^2/p_{KK}{}^I(A). \quad (20)$$

D. ft Values in β-Decay

The reduced transition probability for a Fermi transition operator $\mathfrak{D}_F(\lambda,\mu)$ corresponding to the degree of forbiddenness λ is given by[12]

$$D_F(\lambda)=\sum_{\mu M'}|\langle\Psi_{M'K'}{}^{I'}|\,\mathfrak{D}_F(\lambda,\mu)\,|\Psi_{MK}{}^I\rangle|^2=[(2I'+1)/(2I+1)]|\langle I'K'\|\mathfrak{D}_F(\lambda)\|IK\rangle|^2. \quad (21)$$

Similarly one can define the corresponding quantity for Gamow-Teller (GT) transition operator. The comparative ft values can then be expressed in terms of these reduced transition probabilities.[12] Let us consider a GT operator

$$\mathfrak{D}_{GT}(\lambda,\mu)=S(\lambda)\sum_{i=1}^{A}[\boldsymbol{\sigma}_i\cdot\boldsymbol{\nabla}_i(r_i{}^{\lambda+1}Y_{\lambda+1,\mu}(i))]\tau_\pm{}^i, \quad (22)$$

where the isospin operator $\tau_\pm$ transforms proton into neutron and vice versa. σ_i are the spin operators and $S(\lambda)$ is a constant.[12] We observe that this operator has the same form as the second term in $B_m(\lambda+1,\mu)$ in Eq. (7) except that there is a multiplicative factor $S(\lambda)\tau_\pm{}^i$ instead of $g_s'(1-\tau_3{}^i)$. Therefore the many-particle reduced matrix element $\langle I'K'\|\mathfrak{D}_{GT}(\lambda)\|IK\rangle$ can easily be obtained from Eqs. (5) and (9). There is a difference, however, namely, that the sum over i and

[11] G. R. Satchler, Ann. Phys. **3**, 275 (1958); J. B. French and B. J. Raz, Phys. Rev. **104**, 1411 (1956).

[12] S. G. Nilsson, Kgl. Danske Videnskab. Selskab, Mat. Fys. Skrifter **29**, No. 16 (1955).

k in Eq. (5) must be over all the protons and neutrons, respectively, instead of all the neutrons only.

To conclude this section, it is worth remarking that if we use the definition of the many-particle reduced matrix element given in Eq. (4) and approximate it with only the $\mu'=0$ term, then the expressions for all the operators that we considered above become very similar to the corresponding expressions obtained in the strongly deformed nuclear model of Bohr and Mottelson.

III. APPLICATIONS

In order to test the projected wave functions, we have calculated the magnetic moments, quadrupole moments, and lifetimes of the states of nuclei in the $2s$-$1d$ shell. The electromagnetic transition probabilities have also been computed. We have considered about 20 nuclei ranging from ^{19}F to ^{37}Cl. In all these calculations we have treated all the particles outside the ^{16}O core. The effective two-body interaction employed in the calculations is the Rosenfeld mixture with Yukawa radial dependence:

$$v(i,j)=\tfrac{1}{3}\tau_i\cdot\tau_j(0.3+0.7\sigma_i\cdot\sigma_j)V_0\frac{\exp(-r_{ij}/\mu)}{(r_{ij}/\mu)}.$$

In all cases the calculations were carried out using $V_0=45$ MeV, $\mu=1.37$ F, and the oscillator size-parameter $(\hbar/M\omega)^{1/2}=1.65$ F in computing the two-body matrix elements of the interaction. The single-particle spacings of $d_{5/2}$, $s_{1/2}$, and $d_{3/2}$ are fixed by the strength $\alpha=-2.48$ MeV of the spin-orbit force. We have specifically taken the same parameter values as in the earlier paper[5] because they were found to reproduce an over-all fair agreement between the calculated and experimental low-lying excited spectra and the binding energies of the nuclei in this shell. More trust can be placed in the interaction with these pertinent parameters, and also in the projection technique, if the electromagnetic properties are as fairly reproduced as the energy spectra and the binding energies of nuclei. We stress again that we have not attempted a detailed fit for each nucleus by varying any parameter.

There are[13] a considerable number of experimental data available on the ground-state magnetic moments, though the corresponding information on quadrupole moments is scarce. The magnetic moments of many odd-A nuclei have large deviations from the single-particle Schmidt values. The most conspicuous cases are ^{23}Na, ^{25}Mg, and ^{29}Si for which the experimental ground-state magnetic moments (in units of nuclear magnetons) are 2.22, -0.85, and -0.56 respectively, whereas the Schmidt values are 0.12, -1.91, and -1.91. Recently, magnetic moments of some odd-A nuclei were calculated by Ripka and Zamick[14] by assuming that the last odd nucleon is coupled to a deformed Hartree-Fock core of the even nucleus. In this simplified phenomenological model, by assuming $g_R=0.5$, they get reasonable agreement with experiment in a few odd-A nuclei that they have considered in this region. In our calculations, we do not have to make any simplified model, since we can treat all the nucleons in the system and calculate all the electromagnetic properties. However, as mentioned earlier in the introduction, we may have to attribute an effective charge to the protons and neutrons, since we are neglecting the ^{16}O core and treating only the particles in the $2s$-$1d$ shell.

TABLE I. The Schmidt (sp) calculated and experimental values of the magnetic moment (in units of nuclear magnetons) for the nuclear state with spin J (second column) are tabulated in the third, fourth, and fifth columns, respectively. The sixth and seventh columns, respectively, give the quadrupole moments calculated with $e_p=e$, $e_n=0$, and with $e_p=1.5e$, $e_n=0.5e$ (see text); the last column gives the experimental quadrupole moments. The tabulated quadrupole moments are in units of $e\times10^{-24}$ cm^2.

Nucleus	J	μ_{sp}	μ_{calc}	μ_{expt}	$Q_{calc}^{(1)}$	$Q_{calc}^{(2)}$	Q_{expt}
^{19}F	$\frac{1}{2}$	2.79	2.89	2.63	0	0	
	$\frac{3}{2}$		-1.58		-0.026	-0.06	
	$\frac{5}{2}$		3.78	3.69	-0.04	-0.09	
^{20}F	2	1.73	1.54	2.09	0.03	0.08	
^{19}Ne	$\frac{1}{2}$	-1.91	-2.03	-1.89	0	0	
^{20}Ne	2		1.08		-0.07	-0.14	
^{21}Ne	$\frac{3}{2}$	0.85	-0.57	-0.66	0.047	0.097	0.093
	$\frac{5}{2}$		0.22		-0.02	-0.04	
^{23}Ne	$\frac{5}{2}$	-1.91	-0.71		0.08	0.16	
^{22}Na	3	1.73	1.75	1.75	0.11	0.22	
^{23}Na	$\frac{3}{2}$	0.12	2.11	2.22	0.05	0.10	0.097
	$\frac{5}{2}$		2.09		-0.015	-0.03	
^{24}Na	4	1.73	1.59	1.69	0.13	0.24	
^{24}Mg	2		1.10		-0.08	-0.16	
^{25}Mg	$\frac{5}{2}$	-1.91	-0.58	-0.85	0.09	0.18	0.22
	$\frac{7}{2}$		0.72		0.01	0.03	
	$\frac{1}{2}$		0.25		0	0	
	$\frac{3}{2}$		1.12		-0.06	-0.12	
^{25}Al	$\frac{5}{2}$	4.79	3.37		0.08	0.16	
	$\frac{7}{2}$		3.14		0.03	0.04	
	$\frac{1}{2}$		0.35		0	0	
	$\frac{3}{2}$		0.34		-0.06	-0.12	
^{26}Al	5		2.77		0.11	0.22	
^{27}Al	$\frac{5}{2}$	4.79	3.61	3.64	0.07	0.12	0.15
^{28}Si	2		1.11		0.10	0.20	
^{29}Si	$\frac{1}{2}$	-1.91	-0.38	-0.55	0	0	
	$\frac{3}{2}$		1.93		0.07	0.13	
^{30}P	1		0.40		0.02	0.04	
^{31}P	$\frac{1}{2}$	2.79	1.62	1.13	0	0	
^{32}P	1		-0.39	-0.25	-0.02	-0.04	
^{33}S	$\frac{3}{2}$	0.85	0.54	0.64	-0.015	-0.04	-0.06
^{35}S	$\frac{3}{2}$	0.85	0.65	1.00	0.005	0.03	0.05
^{35}Cl	$\frac{3}{2}$	0.85	0.73	0.82	-0.04	-0.09	-0.08
^{37}Cl	$\frac{3}{2}$	0.85	0.35	0.68	-0.04	-0.06	-0.06

The calculated values of the magnetic moment μ (in units of nuclear magnetons) and the quadrupole moment Q (in units of $e\times10^{-24}$ cm^2) are tabulated in Table I below. The agreement between the calculated and the experimental values of magnetic moments is

[13] I. Lindgren, J. Lindskog, P. Sparrman, and T. Sandstrom, *Perturbed Angular Correlations* (North-Holland Publishing Company, Amsterdam, 1964).

[14] G. Pipka and L. Zamick, Phys. Letters **23**, 347 (1966).

TABLE II. The calculated and the experimental $B(E2)$ values (in units of $e^2\times10^{-48}$ cm^4) for an electromagnetic transition between the initial state (spin J_i) and the final state (spin J_f) are tabulated in the fourth and fifth columns, respectively. The ratio of the calculated $B(E2)$ value to the single-particle estimate is given in the sixth column. The intensity ratio of the $E2$ to $M1$ transition is tabulated in the seventh column. The last two columns give the calculated and the experimental half-lives (in seconds) of the states (spin J_f), respectively; the multiplying factor 10^{-n} is indicated by $(-n)$ in both these columns.

Nucleus	J_i	J_f	$B(E2)_{calc}$	$B(E2)_{exp}$	$\frac{B(E2)_{calc}}{B(E2)_{sp}}$	$\frac{T(E2)}{T(M1)}\times100$	$\tau_{calc}(J_f)$	$\tau_{exp}(J_f)$
^{19}F	$\frac{1}{2}$	$\frac{5}{2}$	0.005	0.005	3.2	∞	11.0(−8)	8.7(−8)
	$\frac{1}{2}$	$\frac{3}{2}$	0.004		2.4	0.6	3.1(−14)	
^{20}Ne	0	2	0.024	0.047	14.0	∞	10.9(−13)	5.3(−13)
	2	4	0.010		6.3	∞	7.9(−14)	5.3(−14)
^{21}Ne	$\frac{3}{2}$	$\frac{5}{2}$	0.012	0.025	6.9	0.1	1.3(−12)	
	$\frac{3}{2}$	$\frac{7}{2}$	0.006		3.7	∞	1.4(−14)	
	$\frac{5}{2}$	$\frac{7}{2}$	0.007		3.8	0.4		
^{23}Na	$\frac{3}{2}$	$\frac{5}{2}$	0.014	0.011	7.2	0.1	4.0(−13)	10.0(−13)
	$\frac{3}{2}$	$\frac{7}{2}$	0.007		3.7	∞	6.3(−15)	
	$\frac{5}{2}$	$\frac{7}{2}$	0.007		3.6	0.7		
^{24}Mg	0	2	0.030	0.054	15.0	∞	19.0(−13)	10.0(−13)
	2	4	0.014		7.1	∞	4.5(−14)	
^{25}Mg	$\frac{5}{2}$	$\frac{7}{2}$	0.012		5.6	0.7	0.6(−14)	1.7(−14)
	$\frac{5}{2}$	$\frac{9}{2}$	0.004		1.9	∞		
	$\frac{7}{2}$	$\frac{9}{2}$	0.006		2.9	0.7	0.5(−14)	
^{25}Al	$\frac{5}{2}$	$\frac{7}{2}$	0.009		4.1	0.5		
^{25}Al	$\frac{5}{2}$	$\frac{9}{2}$	0.003		1.3	∞		
	$\frac{7}{2}$	$\frac{9}{2}$	0.007		3.4	0.4		
^{28}Si	0	2	0.018	0.027	7.0	∞	8.9(−13)	5.1(−13)
	2	4	0.20		8.0	∞		
^{29}Si	$\frac{1}{2}$	$\frac{3}{2}$	0.016		6.1	0.8	0.3(−13)	1.0(−13)
	$\frac{1}{2}$	$\frac{5}{2}$	0.024		9.0	∞		
	$\frac{3}{2}$	$\frac{5}{2}$	0.004		1.4	1.0		
^{31}P	$\frac{1}{2}$	$\frac{3}{2}$	0.006	0.011	2.0	1.1	0.9(−13)	1.5(−13)
	$\frac{1}{2}$	$\frac{5}{2}$	0.008		2.9	∞	3.7(−13)	3.1(−13)
	$\frac{3}{2}$	$\frac{5}{2}$	0.003		1.0	4.0		

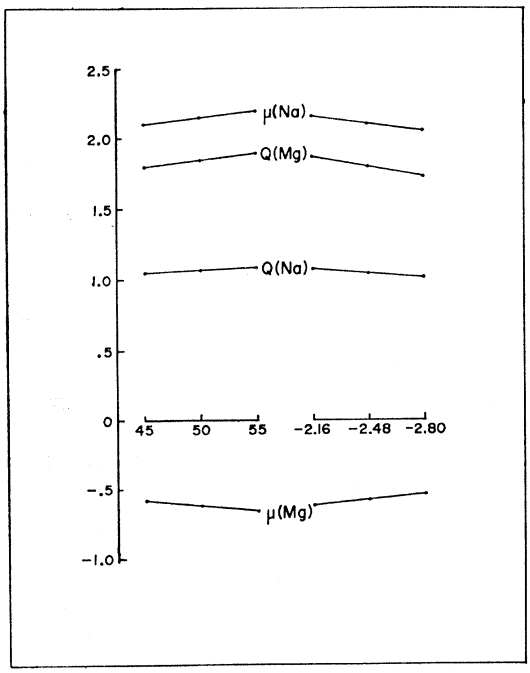

FIG. 1. The variation of the magnetic moment μ (in units of nuclear magneton) and the quadrupole moment Q (in units of $e\times10^{-25}$ cm^2) with V_0 (on the left) and α (on the right) for ^{23}Na and ^{25}Mg. V_0 is varied from 45–55 MeV, and α is varied from 2.16–2.80 MeV.

fair to good over the whole region; the two cases in which there is a considerable disagreement are ^{31}P and ^{37}Cl. However, in the case of ^{31}P, the prolate and oblate HF minima are very close, namely −116.79 MeV and −116.73 MeV, respectively, and the magnetic moments of the $J=\frac{1}{2}$ states projected from the two HF states are 0.62 and 1.62, respectively. The proximity of the two HF states makes the calculated value unreliable. It may be noted that the average of the two values is very close to the experimental magnetic moment. The quadrupole moments Q are calculated by taking the proton charge $e_p=e$, and the neutron charge $e_n=0$; and also with $e_p=1.5e$ and $e_n=0.5e$. As we see from Table I, the agreement between the experimental and calculated values with the latter set of effective charges is quite good over the whole mass region. The additional charge of $0.5e$ attributed to both types of particles is in accordance with the expected Z/A dependence.[6]

The reduced transition probabilities $B(E2)$ for electric quadrupole transitions are calculated by taking the effective charges $e_p=1.5e$ and $e_n=0.5e$. The calculated $B(E2)$ values (in units of $e^2\times10^{-48}$ cm^4) are tabulated in Table II. In the same table, the calculated half-lives of some nuclear states are also tabulated. Since the experimental information on $B(E2)$ and half-life measurements is scarce, we have tabulated only those few cases wherein experimental data are available. From

Table II, it is clear that the calculated $B(E2)$ values are quite good, and at the worst are off by a factor of $\frac{1}{2}$. This is certainly encouraging. The enhancement ratio of the calculated $B(E2)$ to the single-particle estimate varies in the range 2–15. The agreement between the calculated and the experimental half-lives of the states is quite fair. From the calculated intensity ratio of $E2$ to $M1$ transitions, the transitions from the first excited state to the ground state are almost pure $M1$ type in all odd-A nuclei studied.

Though we are keeping V_0 and α fixed for all the nuclei, the effect of the variation of these parameters on the quadrupole and magnetic moment has been studied in case of two nuclei ^{23}Na and ^{25}Mg. This is shown in Fig. 1. It is seen that the magnitudes of Q as well as μ increase with increasing V_0 and decrease with increasing α. However, the variation is slow and quite smooth.

IV. CONCLUSION

A formulation to calculate the electromagnetic properties of nuclei, the form factors in electron scattering, ft values in β decay, and the reduced widths of nuclear states in the direct reaction has been developed, in order to test the nuclear wave functions obtained from a determinantal HF state by the projection technique. Employing a phenomenological internucleon interaction in the form of a Rosenfeld mixture with Yukawa radial dependence, we have calculated the quadrupole and magnetic moments, $B(E2)$ values, and half-lives of nuclear states in a number of nuclei in the sd shell. In view of the fact that we have kept all the parameters fixed, the agreement obtained between the experimental and calculated values over the whole region of the sd-shell nuclei is quite good. It should also be mentioned at this stage that the excited spectra, the binding energies,[5] and the electromagnetic properties of a large number of nuclei in a region are successfully explained by treating all the particles in the system. We also plan to calculate the other nuclear properties described in this paper.

It should, however, be mentioned that since we started from a determinantal HF state for neutrons and protons together, in certain cases it may happen that our projected wave functions do not have a good isospin quantum number. We believe that because of the variational nature of the HF state, the admixture of the excited isospin state would be quite small. It may also be mentioned that our restriction in the HF calculations to orbitals in the sd shell may not be a good approximation for when the total number of nucleons is large. We plan to investigate these points in the near future.

PHYSICAL REVIEW VOLUME 159, NUMBER 4 20 JULY 1967

Energy Levels and Electromagnetic Transitions in N^{15} from the $C^{13}(He^3,p\gamma)N^{15}$ Reaction*

G. W. PHILLIPS,† F. C. YOUNG, AND J. B. MARION
University of Maryland, College Park, Maryland

(Received 13 March 1967)

Excited states of N^{15} have been studied by the $C^{13}(He^3,p\gamma)N^{15}$ reaction. Proton spectra were measured with a magnetic spectrometer at two angles for He^3 energies of 2 and 5 MeV. Excitation energies of 9.054±0.004, 9.225±0.003, 9.829±0.004, and 10.072±0.004 MeV were obtained for levels in N^{15}. Electromagnetic branching ratios were measured for levels at 8.31, 8.57, 9.05, 9.16, 9.22, 9.76, 9.83, 9.93, 10.07, and 10.45 MeV. A comparison was made with theoretical branching ratios calculated from shell-model wave functions for levels at 8.31, 8.57, 9.05, and 9.93 MeV. Measured branching ratios for the first three of these levels agree with calculated ratios for shell-model levels of $J^\pi=\frac{1}{2}^+$, $\frac{3}{2}^+$, and $\frac{1}{2}^+$, respectively. Proton–γ-ray angular-correlation measurements for levels at 9.05, 9.16, and 9.22 MeV indicate $J=\frac{3}{2}$ for the 9.16-MeV state, $J=\frac{1}{2}$ or $\frac{3}{2}$ for the 9.05-MeV level, and $J=\frac{3}{2}$ (90% probability) or $J=\frac{1}{2}$ (10% probability) for the 9.22-MeV level.

I. INTRODUCTION

THE mirror nuclei, N^{15} and O^{15}, are of considerable theoretical interest because in the shell model their lowest-order configurations have only a single hole within the closed $(1s)^4(1p)^{12}$ shell. Thus, shell-model calculations for the low-lying levels are relatively straightforward and are expected to agree reasonably well with experiment. Apart from the Z projection of the isobaric-spin quantum number, the theoretical treatment of N^{15} and O^{15} is identical (neglecting Coulomb-energy effects). Where spins and parities are known, it should be possible to identify experimental levels in N^{15} with their isobaric analog levels in O^{15} which have theoretical wave functions that differ only in T_z.

* Research supported in part by the U. S. Atomic Energy Commission.

† Present address: University of Washington, Seattle, Washington.